



University of Genoa, Italy
The Electrical, Electronics, Telecommunication Engineering and
Naval Architecture Department

Doctoral Thesis Dissertation

Ship Motions and Added Resistance with a BEM in frequency and time domain

Emanuela Ageno

Abstract

This thesis is focused on the calculation of ship motions and on the evaluation of added resistance in waves. A partial desingularized panel method based on potential theory has been developed.

Rankine sources are distributed on the hull and at small distance above the free surface.

In such way only the free surface is desingularized. This choice allows to consider also thin hull shapes at the bow where desingularization could cause numerical problems.

The main advantage of this approach leads to reduce the computational time, especially when non linear effects are considered, provided an adequate source-panel center vertical distance is selected.

The fluid domain boundaries have been represented as a structured grid consisting of flat quadrilater panels.

In the linear case the boundary conditions have been applied on the mean body wetted surface and the free-surface is considered at the calm water level. By using an Eulerian time-stepping integration scheme the kinematic and dynamic boundary conditions are updated on the free-surface at every time-step. After the potential is obtained, the pressure on the mean hull surface can be calculated and forces and moments can be determined by integrating the pressure on the body surface.

Therefore in two-dimensional environment an introduction of non-linear effects has been analysed. In particular a 2D body exact method has been developed.

The added resistance is determined by a near field method integrating the second-order pressure on the body surface. Then it is corrected using a semi-empirical method to allow to consider the wave reflection of short waves.

The adequacy of the results has been verified applying the code to different test cases and comparing the numerical output with experimental data available in literature. Furthermore in order to discuss the improvements obtained with this present method the results have been compared with another numerical method in frequency domain.

Contents

Contents	v
List of Figures	vii
List of Tables	xi
Chapter 1 Introduction	1
1.1 Overview	1
1.2 Background	2
Chapter 2 Mathematical formulation and outlines of numerical method in FD	9
2.1 The physical origin of added resistance	9
2.2 State of the art of added resistance	12
2.2.1 Far Field method	13
2.2.2 Near Field method.....	22
2.2.3 Analysis of non-stationary wave field	29
Chapter 3 Details of the numerical approaches in FD	30
3.1 The added resistance due to ship motion-Near Field methods	30
3.2 The added resistance due to reflected wave at the bow	33
Chapter 4 Mathematical Formulation and outlines of numerical method in TD	36
4.1 Boundary value problem and equation of motion.....	36
4.2 The mathematical formulation for the 3D linear problem	41
4.3 The mathematical formulation for the added resistance in TD.....	44
4.4 The mathematical formulation for the 2D body exact problem.....	46
Chapter 5 Details of the numerical approaches in TD	49
5.1 The indirect method (with partial desingularization) in 3D.....	49
5.2 Time-stepping in 3D	53
5.3 The indirect method (with partial desingularization) in 2D Body exact	53
5.4 Time-stepping in 2D Body Exact	56
Chapter 6 Applications and numerical results	58
6.1 The Added Resistance results in FD	58
6.1.1 The KCS container ship	58
6.1.2 A Fast catamaran.....	64
6.1.3 The DUT catamaran.....	68

6.2	The 3D BEM linear and added resistance results TD	78
6.2.1	The Friesland hull	78
6.2.2	The Serie 60 hull	93
6.2.3	The Wigley hull III	99
6.2.4	The KCS hull	105
Chapter 7	The 2D body exact TD results.....	107
Chapter 8	Conclusions	115
References	117

List of Figures

Figure 2.1: Comparison between total added resistance and viscous component (from Block,1993)..... 10

Figure 2.2: Transfer functions of pitch and added resistance (from Block, 1996) 11

Figure 2.3: Transfer function of added resistance indicating region of large extra resistance (from Block, 1996)..... 12

Figure 2.4: Components of added resistance (from Bertram, 1996)..... 13

Figure 2.5: Energy control surface (from Maruo, 1963) 14

Figure 2.6 15

Figure 2.7 17

Figure 2.8 23

Figure 3.1: Example of Kriso’ s panel system 31

Figure 3.2: Summary of necessary steps..... 32

Figure 3.3: Coordinate system for the short waves range added resistance calculation methods (from Papanikolaou, 2009) 33

Figure 3.4 Definition of the bluntness coordinate [adapted from Kuroda et al., 2008] 34

Figure 4.1: The two different reference systems. 37

Figure 4.2: Components of added resistance on S175 containership: $F_n=0.20$, wave heading angle= 180° (from Kim, 2010) 45

Figure 4.3: Radiation and diffraction components of added resistance on S175 containership (from Kim, 2010) 46

Figure 4.4 Reference system..... 47

Figure 5.1: Desingularized sources (only free-surface)..... 51

Figure 5.2: The two-dimensional panels distribution and body-exact fluid domain. 55

Figure 6.2: Comparison of heave motion between experimental data and numerical results. 61

Figure 6.4: Comparison of the added resistance between experimental data and numerical results. 62

Figure 6.5: BEM results with and without the high frequency correction..... 63

Figure 6.6: Components of added resistance containership KRISO $F_n = 0.26$ 63

Table 6.2: Particulars of the Fast Catamaran (Model scale) 64

Figure 6.7: Perspective view of the Catamaran showing the panel mesh used for seakeeping computations. 65

Figure 6.8: Numerical vs experimental non dimensional RAO of heave motion for the fast catamaran ($s/L=0.4$)	66
Figure 6.9: Numerical vs experimental non dimensional RAO of pitch motion for the fast catamaran ($s/L=0.4$)	66
Figure 6.10: Comparison of the experimental (EFD) and numerical (BEM) prediction of the added resistance for the NPL catamaran advancing in head waves at $Fn = 0.50$	67
Figure 6.12: Comparison of the experimental and numerical RAOs for heave for the DUT catamaran. $Fn = 0.6, \beta = 180^\circ$	69
Figure 6.13: Comparison of the experimental and numerical RAOs for heave for the DUT catamaran. $Fn = 0.6, \beta = 180^\circ$	70
Figure 6.14: Comparison of the experimental and numerical RAOs for heave for the DUT catamaran. $Fn = 0.6, \beta = 135^\circ$	70
Figure 6.15: Comparison of the experimental and numerical RAOs for pitch motions for the DUT catamaran. $Fn = 0.6, \beta = 135^\circ$	71
Figure 6.16: Comparison of the experimental and numerical RAOs for roll motions for the DUT catamaran. $Fn = 0.6, \beta = 135^\circ$	71
Figure 6.17: Added resistance against non-dimensional wave circular frequency. Top to bottom $\beta = 180^\circ$ and $\beta = 135^\circ$. Effect of Fn	73
Figure 6.18: Polar-plot of the heave RAOs for the selected catamaran for head ($\beta = 180^\circ$) to beam ($\beta = 90^\circ$) regular waves. Top to bottom: $Fn = 0.2; 0.4; 0.6$. Radial coordinate: wave length to ship length ratio λL . Polar coordinate: ship-wave heading angle β in degrees.....	74
Figure 6.19: Polar-plot of the roll RAOs for the selected catamaran for head ($\beta = 180^\circ$) to beam ($\beta = 90^\circ$) regular waves. Top to bottom: $Fn = 0.2; 0.4; 0.6$. Radial coordinate: wave length to ship length ratio λL . Polar coordinate: ship-wave heading angle β in degrees.....	75
Figure 6.20: Polar-plot of the pitch RAOs for the selected catamaran for head ($\beta = 180^\circ$) to beam ($\beta = 90^\circ$) regular waves. Top to bottom: $Fn = 0.2; 0.4; 0.6$. Radial coordinate: wave length to ship length ratio λL . Polar coordinate: ship-wave heading angle β in degrees.....	76
Figure 6.21: Polar-plot of the added resistance for the selected catamaran for head ($\beta = 180^\circ$) to beam ($\beta = 90^\circ$) regular waves. Top to bottom: $Fn = 0.2; 0.4; 0.6$. Radial coordinate: wave length to ship length ratio λL . Polar coordinate: ship-wave heading angle β in degrees.	77
Figure 6.22: 3D grid of Friesland	78
Figure 6.23: Added Mass coefficient for Friesland at $Fn = 0.15$, heave due to heave	81
Figure 6.24: Damping coefficient for Friesland at $Fn = 0.15$, heave due to heave.....	81
Figure 6.25: Added Mass coefficient for Friesland at $Fn = 0.15$, pitch due to heave	82
Figure 6.26: Damping coefficient for Friesland at $Fn = 0.15$, pitch due to heave	82
Figure 6.27: Added Mass coefficient for Friesland at $Fn = 0.15$, pitch due to pitch	83
Figure 6.28: Damping coefficient for Friesland at $Fn = 0.15$, pitch due to pitch	83
Figure 6.29: Added Mass coefficient for Friesland at $Fn = 0.15$, heave due to pitch	84
Figure 6.30: Damping coefficient for Friesland at $Fn = 0.15$, heave due to pitch	84

Figure 6.31: Exciting heave force acting on Friesland at $F_n = 0.15$	85
Figure 6.32: Exciting pitch moment acting on Friesland at $F_n = 0.15$	85
Figure 6.33: Friesland RAO for heave motion at $F_n = 0.15$	86
Figure 6.34: Friesland RAO for pitch motion at $F_n = 0.15$	86
Figure 6.35: Added Mass coefficient for Friesland at $F_n = 0.45$, heave due to heave	87
Figure 6.36: Damping coefficient for Friesland at $F_n = 0.45$, heave due to heave.....	87
Figure 6.37: Added Mass coefficient for Friesland at $F_n = 0.45$, pitch due to heave	88
Figure 6.38: Damping coefficient for Friesland at $F_n = 0.45$, pitch due to heave	88
Figure 6.39: Added Mass coefficient for Friesland at $F_n = 0.45$, pitch due to pitch	89
Figure 6.40: Damping coefficient for Friesland at $F_n = 0.45$, pitch due to pitch	89
Figure 6.41: Added Mass coefficient for Friesland at $F_n = 0.45$, heave due to pitch	90
Figure 6.42: Damping coefficient for Friesland at $F_n = 0.45$, heave due to pitch	90
Figure 6.43: Exciting heave force acting on Friesland at $F_n = 0.45$	91
Figure 6.44: Exciting pitch moment acting on Friesland at $F_n = 0.45$	91
Figure 6.45: The Friesland's RAO for heave motion at $F_n = 0.45$	92
Figure 6.46: The Friesland's RAO for pitch motion at $F_n = 0.45$	92
Figure 6.47: 3D grid of Serie 60	93
Figure 6.48: Added Mass coefficient for serie 60 at $F_n = 0.20$, heave due to heave.....	94
Figure 6.49: Damping coefficient for Serie 60 at $F_n = 0.20$, heave due to heave	95
Figure 6.50: Added Mass coefficient for Serie 60 at $F_n = 0.20$, pitch due to pitch.....	95
Figure 6.51: Damping coefficient for Serie 60 at $F_n = 0.20$, pitch due to pitch	96
Figure 6.52: Exciting heave force acting on Serie 60 at $F_n = 0.20$	96
Figure 6.53: Exciting pitch moment acting on Serie 60 at $F_n = 0.20$	97
Figure 6.54: The Serie 60's RAO for heave motion at $F_n = 0.20$	97
Figure 6.55: The Serie 60's RAO for pitch motion at $F_n = 0.20$	98
Figure 6.56: Added resistance for Serie 60 at $F_n = 0.20$	98
Figure 6.57: 3D grid of Wigley hull III	99
Figure 6.58: Added Mass coefficient for Wigley III at $F_n = 0.30$, heave due to heave.....	100
Figure 6.59: Damping coefficient for Wigley III at $F_n = 0.30$, heave due to heave.....	101
Figure 6.60: Added Mass coefficient for Wigley III at $F_n = 0.30$, pitch due to pitch	101
Figure 6.61: Damping coefficient for Wigley III at $F_n = 0.30$, pitch due to pitch	102
Figure 6.62: Exciting heave force acting on Wigley III at $F_n = 0.30$	102
Figure 6.63: Exciting pitch moment acting on Wigley III at $F_n = 0.30$	103
Figure 6.64: The Wigley III's RAO for heave motion at $F_n = 0.30$	103

Figure 6.65: The Wigley III's RAO for pitch motion at $F_n = 0.30$	104
Figure 6.66: Added resistance for Wigley III at $F_n = 0.30$	104
Figure 6.67: The KCS's RAO for heave motion at $F_n = 0.26$	105
Figure 6.68: The KCS's RAO for pitch motion at $F_n = 0.26$	106
Figure 6.69: The KCS's RAO for pitch motion at $F_n = 0.26$	106
Figure 6.70: Reference system of circular section	107
Figure 6.71: Reference system of box section	108
Figure 6.72: Added Mass coefficient for the circular section, heave due to heave	109
Figure 6.73: Damping coefficient for the circular section, heave due to heave	110
Figure 6.74: Added Mass coefficient for the circular section, roll due to roll.....	110
Figure 6.75: Damping coefficient for the circular section, roll due to roll	111
Figure 6.76: Added Mass coefficient for the box section $BT = 8$, heave due to heave	111
Figure 6.77: Damping coefficient for the box section $BT = 8$, heave due to heave	112
Figure 6.78: Added Mass coefficient for the box section $BT = 8$, roll due to roll.....	112
Figure 6.79: Damping coefficient for the box section $BT = 8$, roll due to roll	113
Figure 6.80: Added coefficient for the box section $BT = 8$, roll due to roll for angle 0.05, 0.10 and 0.20rad	113
Figure 6.81: Damping coefficient for the box section $BT = 8$, roll due to roll for angle 0.05, 0.10 and 0.20rad	114

List of Tables

Table 6.1: Design conditions for KCS container ship59
Table 6.3: Main Characteristics of the demi-hull of the DUT catamaran68
Table 6.3: Main Characteristics of Friesland79
Table 6.4: Main Characteristics of Serie 60.....93
Table 6.5: Main Characteristics of Wigley hull III.....99

Chapter 1 Introduction

The study of the ship motions began in the late 19th century and has represented a topic of great interest. An impulse to research on this field arose from the technological innovation of computers, which considered all the different components that influence the seakeeping analysis.

Also the accurate prediction of ship's resistance in waves is nowadays of increased importance, since it greatly influences the ship's performance regarding sustainable service speed and fuel consumption in seaways. This seakeeping-related characteristic typically plays a key role for the performance prediction in operating conditions, as for instance in a weather routing perspective or to evaluate ship maneuvers in waves. Its relevance is rising also at a design phase. In fact it can be related e.g. to Energy Efficiency Index (EEI) evaluations or in designing new fleets for real scenarios since it possibly affects the choices on the power installed on board.

In this chapter the various analytical methodologies to evaluate motions and added resistance in waves, developed in the recent years will be presented and also a summary of the thesis will be provided.

1.1 Overview

In Chapter 2 an overview of the theoretical methods relating to the evaluation of the added resistance due to ship motions in regular waves is provided.

Chapter 3 examines the evaluation of added resistance due to ship motions considering near field methods in frequency domain and the calculation of the added resistance due to wave reflected at the bow using Kuroda's semi-empirical formulation.

In Chapter 4, a quick outline of the Boundary Value Problem (BVP) is presented for the study of a ship advancing in sea waves. The numerical solutions of this approach are described both for the two-dimensional and for the three-dimensional case. Furthermore the near field method in time domain approach is presented.

Chapter 5 discusses in detail the partial desingularization approach for the 3D linear problem and 2D body exact problem. The advantages of this solution procedure compared to the linear methods are underlined. Moreover other relevant aspects in time formulation are analysed as the mesh size, the values of the distance of desingularization, the time stepping for both 3D and 2D body exact method.

In Chapter 6, the applicability of the near field method is presented and in order to validate this methodology the numerical results are compared with the experimental data; then, the three-dimensional approaches, partially desingularized, have been applied to the different hulls and results have been checked with experimental data and with another methodology in frequency domain.

At last the application of the partial desingularized body-exact approach to the two-dimensional sections is shown and the results have been compared with the experimental data freely available in literature and with the two-dimensional linear results.

Finally in Chapter 7 the conclusions, the recommendations and the suggestions for the future research are shown.

1.2 Background

A ship in waves is affected by a higher resistance than that in still water. The difference is known as added resistance, and it is generated by energy dissipation due to ship motion and to reflection of incident waves.

An accurate prediction of added resistance is therefore important for the evaluation of the increased propulsion power to maintain the speed and in view of the related higher emissions. This is the reason why the added resistance problem has been widely studied by many researchers and it is in the focus of a further recent increase of interest. Added resistance may be viewed as the longitudinal component of the steady second-order force so proportional to squared incident wave's amplitude (Storm Tejsen, 1973). Experimentally, added resistances on Series 60 hull and Wigley hull have been measured by Gerritsma and Beukelman (1972), Storm-Tejsen et al. (1973) and Journee (1992), respectively. Two major analytical approach-

es can be used to analyze the problem: far field and near field methods. The far field methods are based on the momentum-conservation theory proposed by Maruo (1960). This approach is not complex and efficacious because there is no necessity to solve a complete boundary value problem to obtain the body pressure, thus the far-field method has been widely used to evaluate the added resistance in real applications. These analysis are well described in ITTC Report (1981). However, in this method there is a limitation in finding a proper control surface, and it is not simple to apply for oblique sea case. Moreover, it is difficult to estimate the added resistances of multiple bodies using the far-field method. Instead the near field method obtains the added resistance by direct integration of the hydrodynamic second-order pressure acting on the wetted ship surface (e.g. Faltinsen (1980), Bertram (1996), Bruzzone & Gualeni (2004), Kim & Kim (2011), Joncquez et al. (2012). Thanks to the significant development of computer power, the near- field method has been acclaimed recently as well as the far-field method. An advantage of the near-field method is that it makes it easier to understand physical phenomena and also it is extendable to the multi-body and nonlinear problems. For example, wave Green function method has been generally applied to the added resistance problem (Grue and Biberg, 1993; Ye and Hsiung, 1997; Choi et al., 2000; Fang and Chen, 2006). These applications are mainly based on three-dimensional frequency-domain approaches. Very recently, Joncquez et al. (2008) analyzed the added resistance problem by using a ship motion program, called AEGIR, which is based on a higher- order Rankine panel method. They compared their computational results with those of momentum-conservation approach. Comparison between computational results based on Neumann–Kelvin and double-body linearization schemes were also realized by Joncquez et al. (2009). Although the success of foregoing studies on the added resistance problem, limited researches can be found that are based on Rankine panel method, with the exception of Joncquez et al. (2008, 2009). However, nowadays, Rankine panel method is widely applied to seakeeping analysis including linear and nonlinear problems.

In this thesis a methodology for the prediction of motions and added resistance by a three-dimensional panel method is presented and its results against experimental data are validated. Furthermore it is known that calculated results of added resistance in short wave frequency range give poor agreement with experimental data. Then a semi empirical procedure by Ku-

roda et al. (2008) for the added resistance in short waves, due to wave reflection at a bow, is applied. Adding this component to the component due to ship motions, the total resistance can be obtained and compared with experimental data.

In order to calculate the added resistance, previously obtained, the ship motions are necessary.

Non-linear effects highly biasing the final output precision mainly cause the complexity regarding the numerical aspects of a ship advancing in waves.

Considering the general formulation of the hydrodynamic problem, the boundary conditions are non linear and the free-surface boundary is unknown a priori.

Several methodologies can be found in literature in order to solve the ship motions issue. They may present various degrees of complexity.

Certainly, attempts in the past were affected by several limitations in computer technology.

In order to simplify the problem different hypothesis were made. An initial two-dimensional boundary value problem was formulated on the base of the strip theory of Korvin-Kroukovsky and Jacobs (1957), valid only for restricted assumptions, and the solution was obtained using a boundary element method such as the one developed by Frank (1967).

For instance, since 1960s in the field of seakeeping computations inviscid methods were developed considering the hypothesis of perfect fluid and irrotational flow. These methods, originally developed in the frequency domain, assumed infinite depth, time harmonic small motions in order to obtain a linear solution of the problem. In the first years of development of this topic, vertical motions were studied using a linear strip theory and the comparison with experimental data, as reported for example in Gerritsma and Beukelman (1967), showed the good accuracy for pitch motions of a slender body results, with an acceptable computational effort.

The early strip theory approach lead to a rational analysis of the method developed by Ogilvie and Tuck (1969) and Sclavounos (1984) and Newman (1978) continued the slender theory standardising the work of Salvesen et al. (1970), who extended the strip method to five degrees of freedom including forward speed effects.

During the years, the development of computer capabilities increased the interest on the practical application of the hydrodynamic methods in order to obtain a realistic simulation of the ship motions in a regular sea state; an initial three-dimensional application was studied and approximated by solving a series of two-dimensional problems in the cross-flow plane.

Successively, in order to evaluate the ship motions the panel methods were developed using Green function technique and assuming the linearized problem. To solve the 3D hydrodynamic boundary value problems with the boundary conditions on the mean wetted body surface and on the calm water surface the Neumann-Kelvin approach was introduced.

In this case, the free-surface and the mean wetted body surface are geometrically described and Green functions are used to solve the boundary value problem. In general, the Green functions are usually used for the solution of inhomogeneous differential equations with specific initial and boundary conditions. In particular, for perturbative methods this approach permits to obtain an approximate solution of the differential equation to solve, but introducing the non-linear effects this method showed some limitations mainly due to the increased computational difficulties. Applications of this method can be found in Inglis and Price (1981), Guevel and Gougis (1982) and Chang and Dean (1986), where, by using a singularity distribution method in frequency domain, numerical results for the motion coefficients, wave resistance and wave forces with forward speed are presented.

Successively Rankine sources Green functions represented a solution to decrease the numerical complexity of the problem, by introduction of the panelization of the fluid domain boundary surfaces and of the distribution of simple sources on which more general free-surfaces conditions may be considered.

In an initial application of this method the body surface and the free-surface remain fixed, so no re-panellization is needed; some examples can be found in Nakos and Sclavounos (1990) and in Bertram (1990), where a Rankine source method is successfully applied to the steady wave problem and in Bruzzone (2003), where a 3D Rankine panel method has been developed and used for the evaluation of motions of high speed marine vehicles.

One of the main aim of the seakeeping analysis is the improvement of the analytical and numerical methods to try to consider as much as possible non linear effects, in order to solve the fully non linear problem. Then due to the complexity of the problem, intermediate methods, where nonlinearities were partially introduced, were developed.

The consideration of non-linear effects directly in the frequency domain results difficult and limited. However, Cummins (1962) introduced the so called 'hybrid or blended methods', based on the impulse functions and on the relation between frequency and time domain through the Fourier transform. Then some results from frequency domain derived. This is a solution that consider the non linearities related to the Froude-Krilov forces and the non linear hydrostatic forces.

An example of a blended approach can be found in Bruzzone et al. (2011), where radiation and diffraction forces are calculated in the frequency domain, while non linear Froude-

Krylov and hydrostatic forces are evaluated in the time domain. This solution permits to evaluate some sources of nonlinearity without increasing very significantly the computational time.

In order to go so far as to consider a fully non-linear approach, a linear panel method completely based in the time domain should be considered rather than in the frequency domain. This is due to the fact that the introduction of non-linear effects in the frequency domain is difficult and doesn't bring particular advantages in the computational effort.

A three-dimensional application of this method in time domain can be found in Beck and Lipis (1987), where, by using time-dependent Green functions on a linearized free-surface, a time domain model for arbitrary shaped slender bodies with forward speed was developed.

In order to introduce the non-linear aspects, the following step was the evaluation of wetted body surface at every time step.

These methodologies were called 'body-exact approaches' and the body boundary condition was satisfied on the instantaneous wetted surface of the body while the free-surface boundary conditions remained linearized. In this case, a new panellization of the body at every time-step should be used in order to update the body surface respect to the wave elevation. Examples can be found also for the two-dimensional case Zhang and Beck (2007).

The first approach to a fully non-linear hydrodynamic problem was developed by Longuet-Higgins and Cokelet (1976), that first introduced the mixed Euler-Lagrange time-stepping scheme for solving two-dimensional fully non linear water wave problems. This method overcame the higher approximations typical of the small amplitude theories, in particular for the study of breaking waves. In this approach, the normal component of the fluid particle velocity is updated at every time-step and the integral equation is solved for this new component of normal velocity. Considering the body boundary condition on the exact wetted surface of the body and the fully non-linear free surface boundary conditions on the deformed surface of the fluid domain a method faster and more accurate than the previous methods, based on the two-dimensional grid, was developed.

In this case, the study of the three-dimensional non-linear problem of the wave generated by a pressure distribution on the free-surface caused by the motions of a submerged or semi-submerged body was solved using MEL methods applied with the boundary integral equation approach. Transient Green singularities were imposed on the hull, as for inst. in Lin and Yue (1990) and in Singh and Sen. (2007), or Rankine singularities on both the hull and on a portion of the free-surface, as for inst. Nakos et al. (1993) or Zhang et al. (2010b). The distribution of the sources on the surfaces determines the methodology used, singular or desingular-

ized. For example, Cao et al (1990, Cao et al. (1991a), and Cao et al. (1991b), used a desingularized boundary integral technique in time domain to study non linear waves.

The use of the desingularized method was principally introduced to reduce computational time, since it simplifies the solution of the influence coefficient matrix, that represents the major computational effort. In fact, in the conventional boundary integral formulations, the singularity of the fundamental solution is placed on the domain boundary. This resulted in the evaluation of singular integrands, which may result in an increased time computations.

Instead, by considering the singularity of the fundamental solution away from the boundary and outside the domain of the problem, the computational effort required for the evaluation of the integrals is reduced. However, it is important to select a proper desingularization distance. Another important difficult to overcome in the solution of desingularized problems is the instability of the free-surface. If the problem is linear and the body surface is considered as the mean body surface, the initial grid is the same for all the time-steps and no regridding is necessary. When an exact-body method is applied, see Zhang et al. (2010b), the body surface change at every time step so a regridding is necessary, with a new distribution of the sources upon the surfaces.

In this thesis, the partial desingularized boundary integral method is examined and an initial linear code has been developed in 3D case, to move forward a non-linear approach. In 2D case a body exact method has been developed as a basis for future development in three-dimensional version.

Chapter 2 Mathematical formulation and outlines of numerical method in FD

2.1 The physical origin of added resistance

The resistance of a ship sailing in still water is composed of a potential part and a viscous part, the magnitudes of which depend on hull form and ship speed. It can be said that they are of equal importance. While the added resistance in the field wave is generally considered to be of potential origin and therefore can neglect the viscous effect. Block (1993) describes this phenomenon in a simple but effective manner.

He derived an approximate expression for the viscous component of the added resistance. He assumes that, considering the same coefficient of viscous resistance, it can be calculated with the same formula that in the stationary case. This is an approximation, since in reality the boundary layer also becomes unstationary, as well as the point of separation of the flow.

The formulation becomes:

$$\bar{R} = 2\pi\rho g C_f \zeta_a^2 \frac{LT}{\lambda} + \frac{V}{\omega} \quad (2.1)$$

where:

C_f = Coefficient of viscous resistance ITTC

T = Immersion of ship

ζ_a = Elevation wave

The values so calculated are compared with the values of added resistance measured experimentally. The result of this comparison is shown in fig. 2.1.

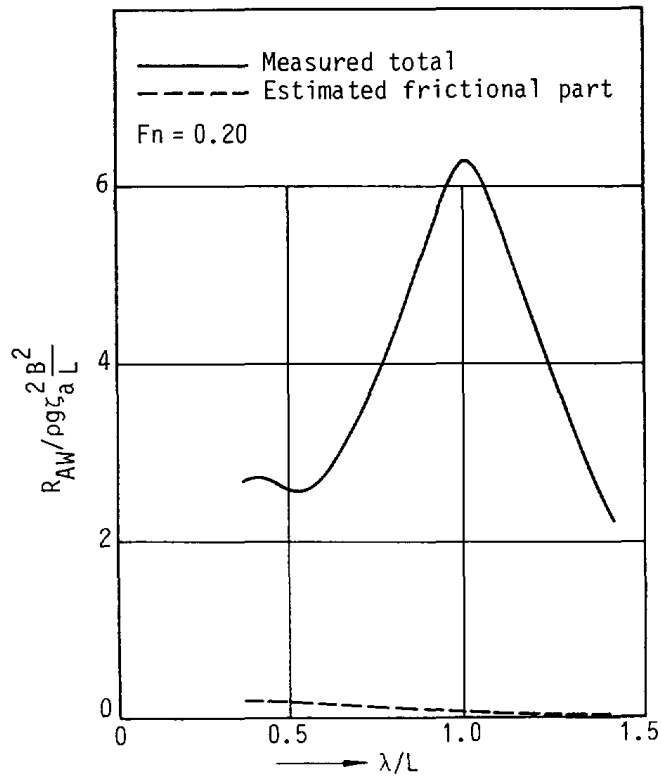


Figure 2.1: Comparison between total added resistance and viscous component (from Block,1993)

Even taking the approximation nature of the formula into account it follows that the mean wave added resistance contains only a small contribution from viscous effects and it is mostly of potential origin. This also means that the results obtained from scale models must follow the Froude scaling law, as for the wave resistance in still water.

Assumed that the added resistance is of potential origin, exactly as the wave resistance in still water also the added resistance is a resistance due to the formation of wave.

In this case the wave field is created by the overlap of the fields generated by the ship motions and the diffraction's waves. All these wave fields are generated by the interaction between the hull and the incident wave field, this phenomenon is already been studied extensively in predict the motions of the ship and this constitutes a solid basis on which to develop techniques for predicting the added resistance.

The wave field in the examination is non-stationary, therefore, when we speak of values for added resistance we make reference to the average value of the resistance added during a period of encounter.

The added resistance is therefore strongly influenced by the ship motions and the experimental data and the numerical calculations confirm this phenomenon. In fact it is possible to find a strong dependence of the added resistance's operator by the transfer functions of the motions. An example is presented in fig. 2.2. This dependence is even more powerful when the wave field generated by motion is responsible of added resistance; for example it is believed that, in case of bow incident waves, the motions responsible for the added resistance

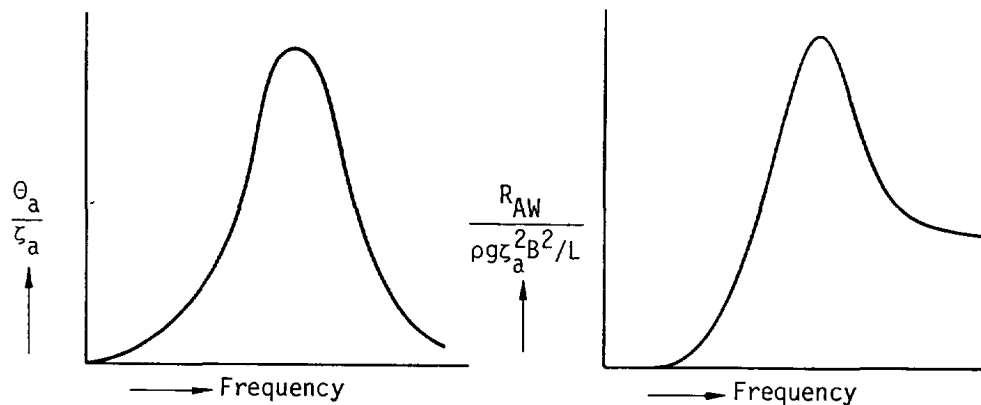


Figure 2.2: Transfer functions of pitch and added resistance (from Block, 1996)

are heave and pitch while all other motions are neglected.

The added resistance is a function of wave length or wave frequency, and attains a maximum value where a dominant ship motion is also maximum.

The ship pitches heavily when the length of waves is equal to the ship's length. The result is large added resistance, as indicated in fig. 2.2

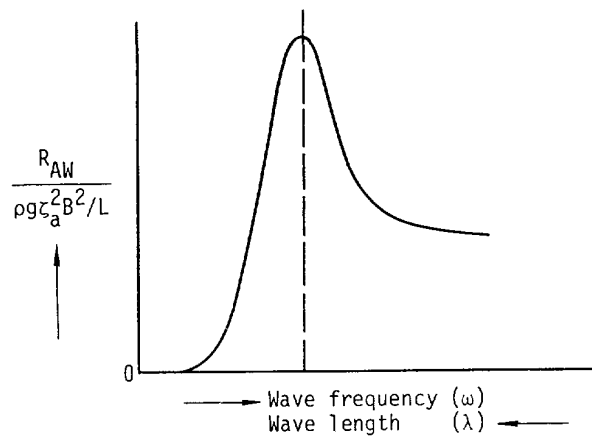


Figure 2.3: Transfer function of added resistance indicating region of large extra resistance (from Block, 1996)

The added resistance is approximately proportional to the square of the wave height. If the wave height increases, then also the water pressure and the surface area on which this pressure acts increase. Their combined integrated effect results in a mean force that increases with the square of the wave height.

2.2 State of the art of added resistance

This section provides an overview of the theoretical methods designed to predict the added resistance due to ship motions in regular waves. Then in section 3.2 methods for estimating the added resistance in short waves due to the reflected wave at the blunt bow, which is not included in theoretical calculation, are presented. In fact it was shown that the total resistance increase of a ship in waves can be evaluated approximately as the sum of the resistance increase due to wave reflection at the bow and the component due to ship motions, as in shown in fig. 2.4.

In general we can distinguish methods called far field and near field, the first calculate the characteristics of the motion at a distance from the ship at least equal to its length while others focus on the motion of the fluid in correspondence of the hull.

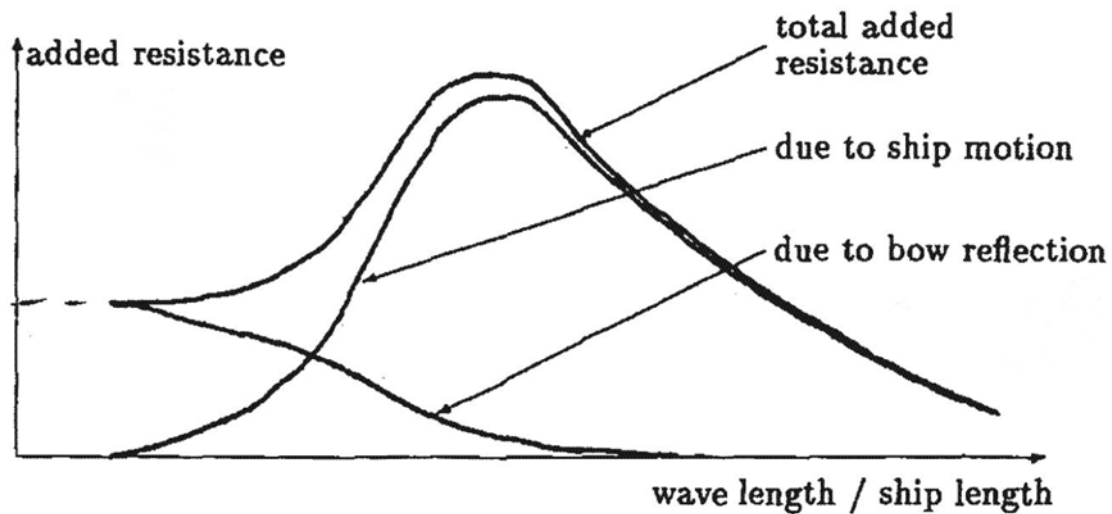


Figure 2.4: Components of added resistance (from Bertram, 1996)

All these methods require knowledge of the motions of the ship and the potential velocity. These quantities can be assessed using 2-D methods, such as strip-theory, still widely used. Currently 3-D methods are spreading, mainly panel methods. In recent years several methods based on non-linear theories have been proposed, which take account of the hull even above the waterline.

2.2.1 Far Field method

The basic idea of this method is to derive the added resistance by applying the laws of conservation of energy and momentum. It was developed in one of the first added resistance theoretical studies by H. Maruo.

When H. Maruo wrote his article (Maruo,1963) no theory was able to describe convincingly the origin of the increase of resistance because the nature of the motion of the fluid around the hull was too complex to allow rigorous mathematical analysis. However, the motion of the fluid away from the hull has characteristics relatively more simple, this allows to apply analytically the equations of conservation of energy and from these relations it can be obtained a formula for calculation of the added resistance.

An analysis of this type has already been applied by Havelock to study the wave resistance of ships in still water. In this case two vertical planes are considered, one in front of the ship that

advances at constant velocity in still water and one behind, farther away. The wave resistance is obtained by the variation of energy of the fluid contained between the two planes.

A similar concept can be applied in the case of a ship that advances in the field of wave, in fact, the added resistance is primarily intended as wave resistance; but in this case the waves generated are also linked to the frequency of the incident wave and the frequency of encounter, therefore, as a control surface it is appropriate to consider a cylindrical surface, with vertical axis, that surrounds the ship.

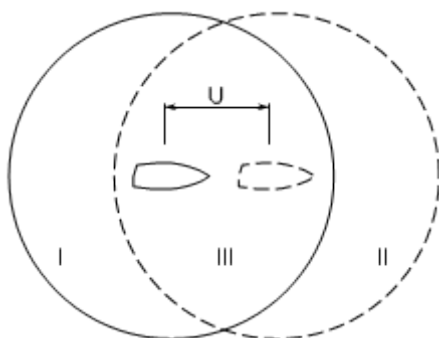


Figure 2.5: Energy control surface (from Maruo, 1963)

Firstly, the case of a ship that advances in still water is considered. The cylindrical surface is assumed fixed in space and the ship moves from left to right with uniform velocity U . After an interval of unit time the ship is at a distance U from its initial position. The change of energy within the cylinder between the initial instant and the final instant, considering the stationary motion of the fluid, is due solely to change of position of the ship.

If instead the cylindrical surface moves with the same speed of the ship, it will be in the C2 position after a interval of unit time (see fig. 2.5) and since the motion is stationary the energy contained in C1 and C2 is identical. The volume indicated as I contains a quantity E_I and E_2 and E_3 are equally identified.

Then the energy variation in the fixed cylinder during a unit time is expressed as:

$$\frac{\partial E}{\partial t} = E_I + E_{III} - (E_{II} + E_{III}) = E_I - E_{II} \quad (2.2)$$

In accordance with the principle of conservation of energy, the energy variation in the fixed cylinder must be supplied from external source. The energy is in part transmitted by the fluid

$\partial W/\partial t$, while the remaining part is given by the ship. When a ship is inclined to a constant velocity U from a drive that overcomes a resistance R , the actual work in a unit time is RU . Therefore the following relation is obtained:

$$R = \frac{1}{U} \frac{\partial E}{\partial t} - \frac{\partial W}{\partial t} \quad (2.3)$$

Where $\partial E/\partial t$ e $\partial W/\partial t$ are determined by the motion of the fluid to the cylindrical surface. In the case where a ship is moving in the wave field motions of the ship and of the fluid are not stationary. The relation just obtained is still valid but the term $\partial E/\partial t$ can not be computed only on the cylindrical surface, also all the terms must be considered as average values in time.

Firstly the situation shown in fig. 2.6 is analysed, where a ship is held in place by a horizontal force, and she is hit by a uniform flow of velocity U at which a train of regular waves is superimposed.

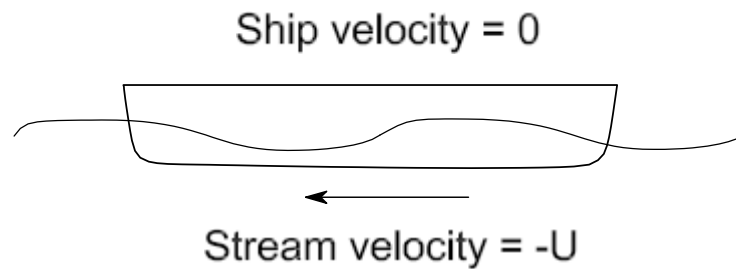


Figure 2.6

From this analysis, a relation that subsequently serves to analyse the real case of a ship that is moving in regular waves, is obtained.

It is assumed that the viscosity of the fluid is zero and the motion is irrotational, then the potential velocity Φ exists and satisfies the Laplace equation.

The Cartesian co-ordinates are taken with the origin on the mean level of water surface, the x-axis is taken in the direction opposite to the velocity of the uniform flow, the z-axis is taken vertically upwards and the y-axis is perpendicular to other axes.

The control surface is the cylindrical surface $S1$ of large radius with a vertical axis through the origin of the co-ordinates, the surface of the hull S and a portion of free surface.

The total energy contained in the domain bounded by the control surfaces is the sum of kinetic and potential energy:

$$E = \iiint \rho \left[\frac{1}{2} (\nabla\Phi)^2 + gz \right] dV \quad (2.4)$$

When the control surfaces move and v_n is the component of velocity in the direction of internal normal the energy variation is given, by transport theorem, as:

$$\frac{dE}{dt} = \frac{\rho}{2} \iiint \frac{\partial}{\partial t} ((\nabla\Phi)^2) dV - \rho \iint \left[\frac{1}{2} (\nabla\Phi)^2 + gz \right] v_n dS \quad (2.5)$$

Using Green's theorem and Bernoulli's equation 2.5 can be written:

$$\frac{dE}{dt} = -\rho \iint \left[\frac{\partial\Phi}{\partial n} \frac{\partial\Phi}{\partial t} + \left(\frac{\partial\Phi}{\partial t} - \frac{p}{\rho} \right) v_n \right] dS \quad (2.6)$$

The boundary conditions are: $v_n = \partial\Phi/\partial n$ on S and S_2 , $p=0$ on S_2 and $v_n = 0$ on S_1 because the cylinder is considered fixed in space. Then:

$$\frac{dE}{dt} = \iint_S p v_n dS - \rho \iint_{S_1} \frac{\partial\Phi}{\partial n} \frac{\partial\Phi}{\partial t} dS \quad (2.7)$$

Taking the mean values in time: $\overline{\partial E/\partial t} = 0$ because the motion is periodic; $\overline{\iint_S p v_n dS}$ is the work done by the ship and since average position of the ship is fixed in space this is also zero.

Then the following relation is found:

$$\iint_{S_1} \frac{\partial\Phi}{\partial n} \frac{\partial\Phi}{\partial t} dS = 0 \quad (2.8)$$

The velocity potential is decomposed as $\Phi = Ux + \varphi$ and using the coordinates cylindrical (R, θ) the previous relation becomes:

$$\int_0^{2\pi} \overline{\int_{-\infty}^{\zeta} \frac{\partial \phi}{\partial t} \left(\frac{\partial \phi}{\partial R} + U \cos \theta \right) dz} = 0 \quad (2.9)$$

Where ζ is the elevation of the free surface.

Now, the real situation of a ship that moves with mean velocity U in regular waves, as shown in Fig. 2.7, is analysed. The coordinate system moves with the ship, the velocity potential in mobile reference is identical to ϕ . The cylinder S_1 moves with the origin of coordinates and then $v_n = -U \cos \theta$ in S_1 .

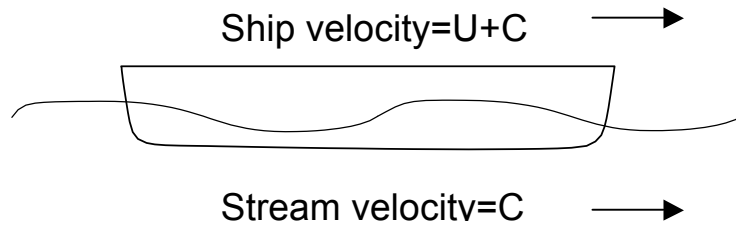


Figure 2.7

In this case the energy variation is:

$$\frac{dE}{dt} = \iint_S p v_n dS - \iint_{S_1} \left[\rho \left(\frac{\partial \phi}{\partial t} - U \frac{\partial \phi}{\partial x} \right) \left(\frac{\partial \phi}{\partial n} - U \cos \theta \right) + \rho U \cos \theta \right] dS \quad (2.10)$$

Taking the average value in time and using the relation (2.8):

$$\begin{aligned} \overline{\iint_S p v_n dS} &= - \overline{\iint_{S_1} \left[\rho U \frac{\partial \phi}{\partial x} \left(\frac{\partial \phi}{\partial n} - U \cos \theta \right) - \rho U \cos \theta \right] dS} \\ &= \rho U \int_0^{2\pi} R d\theta \overline{\int_{-\infty}^{\zeta} \frac{\partial \phi}{\partial x} \frac{\partial \phi}{\partial R} + \left[\frac{\partial \phi}{\partial t} - \frac{1}{2} (\nabla \Phi)^2 - gz \right] \cos \theta dz} \end{aligned} \quad (2.11)$$

The term on the left of the equal is the work done by the ship. The only force that supply this work is the thrust of the ship then the principle of conservation of energy leads to this expression:

$$\overline{\iint_S p v_n dS} = \bar{R}U \quad (2.12)$$

Where \bar{R} is the average resistance in the wave field. Using cylindrical coordinates, by (2.11), the average resistance can be expressed as follows:

$$\bar{R} = \rho U \int_0^{2\pi} R d\theta \overline{\int_{-\infty}^{\zeta} \frac{\partial \varphi}{\partial x} \frac{\partial \varphi}{\partial R} + \left[\frac{\partial \varphi}{\partial t} - \frac{1}{2} (\nabla \Phi)^2 - gz \right] \cos \theta dz} \quad (2.13)$$

Since the motion is periodic:

$$\int_0^{2\pi} R d\theta \overline{\int_{-\infty}^0 \left(\frac{\partial \varphi}{\partial t} - gz \right) \cos \theta dz} = 0 \quad (2.14)$$

Then the equation (2.14) can be rewritten as:

$$\begin{aligned} \bar{R} = \rho \int_0^{2\pi} R d\theta \overline{\int_{-\infty}^0 \left[\frac{\partial \varphi}{\partial x} \frac{\partial \varphi}{\partial R} - \frac{1}{2} (\nabla \Phi)^2 \right] \cos \theta dz} \\ + \rho \int_0^{2\pi} R d\theta \overline{\int_0^{\zeta} \left[\frac{\partial \varphi}{\partial x} \frac{\partial \varphi}{\partial R} - \frac{1}{2} (\nabla \Phi)^2 \right] \cos \theta dz} \\ + \rho \int_0^{2\pi} R d\theta \overline{\int_0^{\zeta} \left[\frac{\partial \varphi}{\partial t} \cos \theta dz \right]} \\ - \frac{1}{2} \rho g \int_0^{2\pi} \overline{\zeta^2} R \cos \theta d\theta \end{aligned} \quad (2.15)$$

The integrals contained in equation (2.15) are developed in power series compared to ζ of lower order, which is a term quadratic of derivative of φ

$$\begin{aligned}\bar{R} = \rho \int_0^{2\pi} R d\theta \int_0^{-\infty} \overline{\frac{\partial \varphi}{\partial x} \frac{\partial \varphi}{\partial R}} - \frac{1}{2} \overline{(\nabla \Phi)^2} \cos \theta dz \\ + \varrho \int_0^{2\pi} \left(\overline{\frac{\partial \varphi}{\partial t} \zeta} - \frac{1}{2} \overline{g \zeta^2} \right)_{z=0} R \cos \theta d\theta\end{aligned}\quad (2.16)$$

The elevation of the free surface is approximated to first order as:

$$\zeta = \frac{1}{g} \left(\overline{\frac{\partial \varphi}{\partial t}} - U \overline{\frac{\partial \varphi}{\partial t}} \right)_{z=0} \quad (2.17)$$

Substituting 2.17 in equation 2.16, the following expression derives:

$$\begin{aligned}\bar{R} = \rho \int_0^{2\pi} R d\theta \int_0^{-\infty} \overline{\frac{\partial \varphi}{\partial x} \frac{\partial \varphi}{\partial R}} - \frac{1}{2} \overline{(\nabla \Phi)^2} \cos \theta dz \\ + \frac{1}{2g} \varrho \int_0^{2\pi} \left(\overline{\frac{\partial \varphi}{\partial t} - U \frac{\partial \varphi}{\partial x}} \right)_{z=0} \left(\overline{\frac{\partial \varphi}{\partial t} + U \frac{\partial \varphi}{\partial x}} \right)_{z=0} \cos \theta R d\theta\end{aligned}\quad (2.18)$$

To solve this equation the potential φ must be known, the boundary conditions for the Laplace equation are the conditions on the free surface and the condition on the rigid surface. These conditions are nonlinear and it's very difficult to find a solution. The solution is approximated solving a linearized problem.

The linearized potential velocity is the sum of φ_w - the potential of the incident regular waves - and φ_d - the potential of disturbance - .

The potential of disturbance is harmonic in external space to the hull so there must be singularities on the surface or inside the ship. The singularities are considered as a source distribution on the surface S.

The following function is considered:

$$H(K, \alpha, t) = \iint_S \sigma(t, x', y', z') \exp k(z' + ix' \cos \alpha + iy' \sin \alpha) dS(x', y', z') \quad (2.19)$$

$\sigma(t, x', y', z')$ where is the density of the sources.

After the oscillations of the ship are damped, the period of the oscillations is the period of encounter. Then $H(k, \alpha, t)$ is a periodic function:

$$H(K, \alpha, t) = H_0(k, \alpha) + P_1(k, \alpha) \cos \omega_e + Q_1(k, \alpha) \sin \omega_e + \dots \quad (2.20)$$

Using conjugate complex numbers it can be written:

$$P_1(k, \alpha) + P_1^*(k, \alpha + \pi) - i[Q_1(k, \alpha) + Q_1^*(k, \alpha + \pi)] = 2H_1(k, \alpha) \quad (2.21)$$

With a few calculations the potential velocity φ_d is expressed as a function of: $H_0(k, \alpha)$, $H_1(k_1, \alpha)$ and $H_2(k_2, \alpha)$

Where:

$$k_{1,2} = k_0 \frac{1 - 2\Omega \cos \alpha \pm \sqrt{1 - 4\Omega \cos \alpha}}{2 \cos \alpha^2} \quad \Omega = \frac{U \omega_e}{g} \quad (2.22)$$

The potential of disturbance is written as $\varphi_d = Re\{\varphi_0 + \varphi_1 e^{-i\omega_e t}\}$. φ_0 is the time-independent part and $\varphi_1 e^{-i\omega_e t}$ is periodic part. Likewise: $\varphi_w = Re\{\varphi_2 e^{-i\omega_e t}\}$.

Considering large-distance asymptotic expression for φ_0 and φ_1 and substituting in 2.18 the following formulation of wave resistance in still water is obtained:

$$R_0 = \rho \int_0^{2\pi} R d\theta \int_0^{-\infty} \left[\frac{\partial \varphi_0}{\partial x} \frac{\partial \varphi_0}{\partial R} - \frac{1}{2} (\nabla \Phi)^2 \cos \theta \right] dz \quad (2.23)$$

Then the increased resistance in the field wave is:

$$\begin{aligned} \Delta R = 2\pi\rho \left\{ \left[\int_{-\pi/2}^{2\pi-\alpha_0} + \int_{\alpha_0}^{\pi/2} - \int_{\pi/2}^{3\pi/2} \right] |H_1(k_1, \alpha)|^2 \frac{k_1(k_1 \cos \alpha - k \cos \chi)}{\sqrt{1 - 4\Omega \cos \alpha}} d\alpha \right\} \\ + 2\pi\rho \left\{ \int_{\alpha_0}^{2\pi-\alpha_0} |H_1(k_2, \alpha)|^2 \frac{k_2(k_2 \cos \alpha - k \cos \chi)}{\sqrt{1 - 4\Omega \cos \alpha}} d\alpha \right\} \end{aligned} \quad (2.24)$$

The determination of the function $H_1(k_1, \alpha)$ is essential in this calculation of added resistance. H. Maruo uses an approximate method using the source distribution.

2.2.1.1 Method of energy radiated

This method has been developed by J. Gerritsma and W. Beukelman. On the basis of past studies on the added resistance, such as the formula of Havelock or a simplified version of the formula 2.24, the authors have considered the added resistance to be the result of the energy dissipated by the ship through the radiated waves of damping.

The following procedure shows how to calculate the radiated energy P during a period of encounter from a ship which oscillates.

$$P = \int_0^T \int_0^L b' V_z^2 dx_b dt \quad (2.24)$$

where:

$b' = b_{33} - V \frac{da_{33}}{dx_b}$ is the sectional damping coefficient

$V_z = z - x_b \theta + V \theta - \zeta^*$ is the relative vertical velocity of water

ζ^* is the effective wave elevation for the section b, in fact for each section wave height is different due to the shape of the itself section, this is a correction to the Froude-Kryloff 's hypothesis who assumes that incident wave field is not affected by the presence of the ship.

It is expressed as follows:

$$\zeta^* = \zeta \left(1 - \frac{k}{y_w} \int_{-T}^0 y_b e^{kz_b} dz_b \right) \quad (2.25)$$

(y_b, z_b) are the points of the section and y_w is the half width at the waterline of the section x_b .

V_z is a harmonic function with amplitude V_{za} and frequency w_e . Then this following expression is obtained:

$$P = \frac{\pi}{w_e} \int_0^L b' V_{za}^2 dx_b \quad (2.26)$$

From energy considerations (Maruo,1963):

$$P = R_{AW}(V + C)T_e = R_{AW}\lambda \quad (2.27)$$

Then the added resistance is found as:

$$R_{aw} = \frac{k}{2w_e} \int_0^L b' V_{za}^2 dx_b \quad (2.28)$$

This method emphasizes the close relation between vertical motions and added resistance, therefore an accurate prediction of added resistance depends on the goodness of calculation of the ship's motions.

2.2.2 Near Field method

These methods, on the other side, leads to the added resistance as the steady second-order force obtained by direct integration of the hydrodynamic, steady second-order pressure acting on the wetted ship surface.

As example of this method is presented in the work done by V. Bertram (1996). This is the frequency domain approach used in this thesis.

A ship that advances with an average velocity U in the harmonic wave of small amplitude is considered. Firstly the motions of the ship are determined using 3-D panel methods, in particular Rankine source methods (RSM). RSM describe the velocity potential by distributing Rankine source over the body and the part of the surrounding free surface.

The total velocity potential is decomposes into the steady potential due to forward motion of the ship in still water, the incoming wave potential, the diffraction potential due to the interaction of the motionless ship with incoming waves and the radiation potentials due to forced motions of the ship. Then the total potential velocity Φ is expressed as:

$$\Phi = \Phi_s + \Phi_{us} = \Phi_s + \phi^d + \phi^w + \sum \phi^i u_i \quad (2.29)$$

This decomposition is justified by the linearization of the problem assuming small wave amplitudes.

Besides the Laplace equation into the flow field, the total potential Φ must satisfy the body and the free surface boundary conditions.

The added resistance is the negative value of the longitudinal component of the forces of the second order:

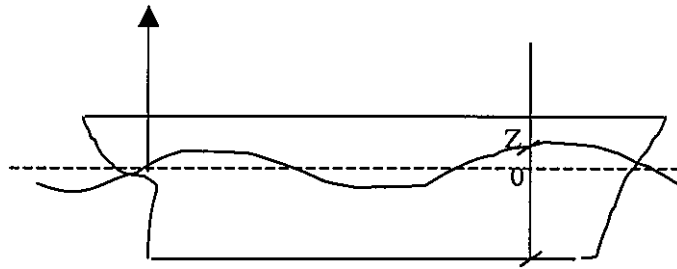


Figure 2.8

$$F_2 = [\int_S p n dS]_2 = \int_c \int_k^z p n dC dZ = \int_c \int_k^0 p n dC dZ + \int_c \int_0^z p n dC dZ \quad 2.30$$

In the first integral the integral on the surface can be replaced by one on the undisturbed surface $S(0)$. Then the following expression is derived:

$$F_2 = \int_{S_0} p n dS_0 + \int_c \int_0^z p n dC dZ \quad (2.31)$$

To capture the effects of forces of second order it must pass from inertial system (\underline{x}) to body fixed (\underline{x}) . (The inertial $0xyz$ system moves uniformly with velocity U . x points in the direction of the body's mean velocity U . z points vertically downwards; The $oxyz$ is fixed at the body and follows its motions.)

$$\underline{\vec{x}} = \underline{\vec{x}} + \underline{\vec{\alpha}} \times \underline{\vec{x}} + \underline{\vec{u}} \quad (2.32)$$

$$\underline{\vec{n}}(\underline{x}) = \underline{\vec{n}}(\underline{\vec{x}}) + \underline{\vec{\alpha}} \times \underline{\vec{n}}(\underline{\vec{x}}) \quad (2.33)$$

where $\vec{\alpha}$ is the rotational motion vector and \vec{u} is the motion vector.

Considering a Taylor expansion of p and making the variation of reference system:

$$\begin{aligned} F_2 &= \left[\int p + \nabla p(\vec{\alpha} \times \vec{x} + \vec{u})(\vec{n} + \vec{\alpha} \times \vec{n}) dS \right]_2 \\ &= \left[\int p \vec{n} + p(\vec{\alpha} \times \vec{n}) + \nabla p(\vec{\alpha} \times \vec{x} + \vec{u}) \vec{n} + \nabla p(\vec{\alpha} \times \vec{x} + \vec{u})(\vec{\alpha} \times \vec{n}) \right]_2 \end{aligned} \quad (2.34)$$

This expression can be rewritten as follows:

$$F_2 = \left[\int (p + \nabla p(\vec{\alpha} \times \vec{x} + \vec{u})) \vec{n} dS + \int (p + \nabla p(\vec{\alpha} \times \vec{x} + \vec{u})) (\vec{\alpha} \times \vec{n}) dS \right]_2 \quad (2.35)$$

The terms that represent the pressure are replaced as follows to secure the second-order terms.

$$F_2 = \left[\int (p_2 + \nabla p_1(\vec{\alpha} \times \vec{x} + \vec{u})) \vec{n} dS + \int (p_1 + \nabla p_0(\vec{\alpha} \times \vec{x} + \vec{u})) (\vec{\alpha} \times \vec{n}) dS \right]_2 \quad (2.36)$$

Where:

p_2 represents a second order pressure term.

p_1 represents a first order pressure term, which combined with the first order terms of the normal or of the movement shall provide second order elements.

p_0 are the zero order elements that however multiply the second order elements due to normal or the movement.

By using Bernoulli equation, Taylor's expansion and the perturbation formulation for the potential:

$$p = -\rho \left(\Phi_t + \frac{1}{2} \nabla \Phi \cdot \nabla \Phi + gz - \frac{1}{2} U^2 \right) \quad (2.37)$$

$$p(\eta) = p(0) + p'(0)\eta + \frac{1}{2} p''(0)\eta^2 \quad (2.38)$$